Journal of Insect Science, (2019) 19(1): 15; 1–11
doi: 10.1093/jisesa/iey134
Research

Molecular Characterization of Two Mitogen-Activated Protein Kinases: p38 MAP Kinase and Ribosomal S6 Kinase From *Bombyx mori* (Lepidoptera: Bombycidae), and Insight Into Their Roles in Response to BmNPV Infection

Azharuddin Muhammad,[1,2,*] Shahzad Toufeeq,[1,2,*] Hai-Zhong Yu,[3] Jie Wang,[1,2] Shang-Zhi Zhang,[1,2] Bing Li,[1,2] Zhen Li,[1,2] Li-Ang Yang,[1,2] Pei Hu,[1,2] Yan Ma,[1,2] and Jia-Ping Xu[1,2,4]

[1]School of Life Sciences, Anhui Agricultural University, Hefei, China, [2]Anhui International Joint Research and Developmental Center of Sericulture Resources Utilization, Hefei, China, [3]National Navel Orange Engineering and Technology Research Center, Gannan Normal University, Ganzhou, China, and [4]Corresponding author, e-mail: jiapingxu@163.com

*These authors equally contributed to this study.

Received 31 October, 2018; Editorial decision 7 December, 2018

Subject Editor: Luc Swevers

Abstract

Proteins p38 map kinase and ribosomal S6 kinase (S6K) as members of mitogen-activated protein kinases (MAPKs) play important roles against pathogens. In this study, Bmp38 and BmS6K were identified as differentially expressed proteins from iTRAQ database. Bmp38 and BmS6K were expressed, and recombinant proteins were purified. The bioinformatics analysis showed that both proteins have serine/threonine-protein kinases, catalytic domain (S_TKc) with 360 and 753 amino acids, respectively. The real-time quantitative polymerase chain reaction (RT-qPCR) results suggest that *Bmp38* and *BmS6K* had high expression in the midgut and hemolymph. The comparative expression level of *Bmp38* and *BmS6K* in BC9 was upregulated than in P50 in the midgut after *Bombyx mori* nucleopolyhedrovirus (BmNPV) infection. Western bolt results showed a positive correlation between RT-qPCR and iTRAQ data for Bmp38, but BmS6K data showed partial correlation with iTRAQ. Injection of anti-Bmp38 and anti-BmS6K serum suggested that Bmp38 may be involved against BmNPV infection, whereas BmS6K may require phosphorylation modification to inhibit BmNPV infection. Taken together, our results suggest that Bmp38 and BmS6k might play an important role in innate immunity of silkworm against BmNPV.

Key words: *Bombyx mori*, *Bombyx mori* nucleopolyhedrovirus, p38 mitogen-activated protein kinase, ribosomal S6 kinase

Mitogen-activated protein kinases (MAPKs) are class of evolutionarily conserved protein with Ser/Thr kinase domain. MAPKs have been widely identified from vertebrates to invertebrates, which involve in different signaling transduction pathways (Roux and Blenis 2004). MAPK family can be classified into three major groups: extracellular signal-regulated kinases (ERKs), C-Jun N-terminal Kinases (JNKs), and p38 MAPKs (Marie Cargnello 2011). In addition, MAPKs are triggered by phosphorylation of conserved TxY motifs present in their Ser/Thr kinase domains. Among them, p38 and ribosomal S6 kinase (S6K) are members of MAPKs play a wide range of functions in various biological processes including apoptosis, pathogen infection, cell differentiation, inflammatory response, UV stress, and environmental stress (Yee et al. 2004, Regan et al. 2009, Fenton and Gout 2011). Both p38 and S6K MAPK homolog have been studied in vertebrates and invertebrates (Han et al. 1998, Fenton and Gout 2011).

Innate immune response is conserved from higher to lower organisms and plays vital role against pathogenic infection (Shahzad et al. 2017). Previous studies have shown that p38 MAPK triggered inflammatory response and initiated innate immune responses in shrimp (He et al. 2013). Moreover, some studied also discovered that p38 MAPKs are also initiated during mammalian viral infection and involve in viral replication (Banerjee et al. 2002, Hirasawa et al. 2003). Wei et al. (2015) revealed that p38 MAPK involved in virus replication during irridovirus infection. p38 MAPKs from *Drosophila* mediated

host defense against bacteria and fungi, as well as p38 pathway involved in stress response (Chen et al. 2010). S6K belongs to AGC family of kinases, which are a direct substrate of ERK1/ERK2 (Tavares et al. 2015). S6K1 and S6K2, homologous of S6K, have been identified in mammals (Gwalter et al. 2009). S6K1 and S6K2 when interact with Kaposi's sarcoma-associated herpesvirus, their kinase activities are increased (Kuang et al. 2008). The loss of S6K in *Drosophila* leads to small cell size and body (Montagne et al. 1999). Evidence suggests that RSK2 participates in innate immune responses, and its knockdown stimulates the growth of influenza virus (Kakugawa et al. 2009).

The silkworm, *Bombyx mori* (Linnaeus), is a model lepidopteran insect with great economic value (Xia et al. 2004). *Bombyx mori* nucleopolyhedrovirus (BmNPV) is a double-stranded DNA virus that exclusively infects the silkworm (Yu et al. 2017b). To date, most silkworm strains are highly susceptible to BmNPV infection, only a few resistant strains are available (Wang et al. 2017). Owing to BmNPV infection, sericulture undergoes serious economic loss every year. However, there are no effective measures available to control BmNPV infection; thus, investigation is needed to explore the interaction between the host and BmNPV to prevent infection.

In the present study, we analyzed *B. mori* p38 MAPK and ribosomal S6 kinase proteins, examined their tissue expression, and evaluated their expression at transcription and translation level in response to BmNPV challenge. Taken together, our results suggest that Bmp38 and BmS6K may involve in BmNPV infection.

Materials and Methods

Bombyx mori Rearing and Virus Preparation

The preservation of silkworm-susceptible strain P50 (LC_{50} = 1.03 × 10^5) and -resistant strain A35 (LC_{50} = 5.90 × 10^7) was performed in Key Laboratory of Sericulture and Anhui Agricultural University, Hefei, China. The near-isogenic line BC9 (LC_{50} = 2.27 × 10^6) was constructed according to protocol of Wang et al. (2017). In brief, susceptible strain P50 were crossed with resistant strain A35, and progeny was repeatedly backcrossed with the P50 for nine generations, and each progeny was screened with BmNPV. Hence, the genetic background of BC9 is much similar to the P50, but BC9 should have the resistant background derived from A35. All larvae were reared as described previously (Yu et al. 2017b). Briefly, fresh mulberry leaves were used to feed larvae. The first- to third-instar larvae were raised in artificial climate chamber at temperature 26 ± 1°C with relative humidity of 75 ± 5% at 12 h day/night cycles, and temperature 24 ± 1°C was used for fourth- and fifth-instar larvae with the same relative humidity and photoperiod as mentioned previously.

BmNPV T3 strain was kept in our laboratory. On the first day of the fifth instar, all larvae were starved for 24 h; 30 silkworm larvae in each of the three independent experiments were administrated 5-μl BmNPV inclusion bodies suspended in water (5 × 10^5/ml) per os, and the control was treated with 5 μl of sterile water. After 24 h, 30 larval midgut were dissected and mixed together to eliminate individual genetic differences; then, the sample was frozen in liquid nitrogen and stored at −80°C for further use.

Investigation of BmNPV Proliferation by Real-Time Quantitative Polymerase Chain Reaction

Total genomic DNA was isolated using midgut of P50 and BC9 infected with BmNPV injection and oral inoculation, and using the genomic DNA extraction kit, the noninfected larvae were isolated at time 6, 12, 24, 48 and 72 hpi (Dalian, Takara, China). To measure the quantity of all DNA samples, a spectrophotometer (Nano-Drop 2000; Thermo Fisher Scientific, New York, NY) was used. To check the purity of all DNA samples, $A_{260/280}$ and $A_{260/230}$ absorbance ratio was used, and 1.0% agarose gel electrophoresis was used to confirm the integrity of DNA. The *GP41* primer was showed in Table 1. *Glyceraldehyde 3-phosphate dehydrogenase* (*GAPDH*; GenBank ABA.43638) gene was used as a reference gene because of its suitability described previously (Guo et al. 2016). The real-time qPCR was performed in a 25-μl reaction mixture containing 12.5 μl of TB Green premix EX Taq (TaKaRa). PCR amplification was performed in triplicate wells. The thermal cycling program was set as denaturation at 95°C for 30 s and 40 cycles of 95°C for 5 s, 60°C for 30 s, and 72°C for 20 s. All these reactions were carried out in 96-well plates with a Multicolour Real-Time PCR Detection System (Bio-Rad, Hercules, CA). $2^{-\Delta\Delta Ct}$ method was used to calculate the relative expression level followed the previously published protocol (Yu et al. 2007). Analysis of variance (ANOVA) and least significance difference (LSD) a posteriori tests were used for statistical analysis by using SPSS software ($P < 0.01$).

Table 1. Primers used in this study

Primers	Sequences of primers (5′–3′)	Purpose
Bmp38-F	TCGGCTGGCATCATTCATAG	RT-qPCR
Bmp38-R	TTCAGTCTCAGTGGGTCTCGC	RT-qPCR
BmS6K-F	AACCACAATACGCAGAACCCA	RT-qPCR
BmS6K-R	TCGCACCACCGAGAATGAA	RT-qPCR
BmGAPDH-F	CATTCCGCGTCCCTGTTGCTAAT	RT-qPCR
BmGAPDH-R	GCTGCCTCCTTGACCTTTTGC	RT-qPCR
Bmp38-F	CGC*GGATCC**CTTACACCTGTAGGTTCCGG (*EcoRI*)	Protein expression
Bmp38-R	CCG*CTCGAG*TTCTGCCGTTATGCGTTTA (*XhoI*)	Protein expression
BmS6K-F	CGC*GGATCC*GCATTCCAAACAGCTGGTA (*EcoRI*)	Protein expression
BmS6K-R	CCG*CTCGAG*GTCTCTTGGCGTTCTACAG (*XhoI*)	Protein expression
GP64-F	GAAGTAGAAACGCCGCATCG	RT-qPCR
GP64-R	GTGGGGTATCAGGCAGCAGT	RT-qPCR
GP41-F	CGTAGTAGTAGTAATCGCCGC	RT-qPCR
GP41-R	AGTCGAGTCGCGTCGCTTT	RT-qPCR
IE-1-F	AGAAGGAGGACGGCAGCAT	RT-qPCR
IE-1-R	TCTCGCCAGAAATCCAATAAAAC	RT-qPCR

*The underline represented restriction enzyme cutting site. RT-qPCR (real-time quantitative polymerase chain reaction).

Identification of Bmp38 and BmS6K, and Bioinformatics Analysis

The iTRAQ-labeling quantitative proteomic technique was used to identify differentially expressed proteins in P50 (susceptible strain) and near-isogenic line BC9 (resistant strain) according to the mass spectra data (Yu et al. 2017b). Finally, Bmp38 and BmS6K were identified based on National Center for Biotechnology Information non-redundant (NCBI-nr) database using basic local alignment search tool. Online ExPASy was used for the analysis of isoelectric point (IP) and molecular weight (MW) of Bmp38 and BmS6K (http://web.expasy.org/compute_pi/). SMART was used for the conserved domain (http://smart.embl-heidelberg.de/). To build the phylogenetic tree MEGA 6.0 software was used, following the neighbor-joining method with 1,000-fold bootstrap (Tamura et al. 2013).

Extraction of Total RNA and cDNA Synthesis

Silkworms were dissected for the collection of the midgut, hemolymph, fat body, integument, head, and silk gland (pathogen challenged) and using TRIzol reagent (Invitrogen, Carlsbad, CA) as per manufacturer's protocol. A Nano-Drop 2000 Spectrophotometer (Thermo Fisher Scientific) was used to determine the concentration, and purification of RNA samples was noticed at $A_{260/280}$. 1% agarose gel electrophoresis was used for checking RNA integrity. According to previous protocol, the RNA samples were then reverse transcribed into cDNA by using Primescript RT Kit with gDNA Eraser (Takara; Yu et al. 2018). Briefly, the concentration was adjusted at 1 µg/µl with nuclear-free water for each RNA sample, and in a 20-µl reaction mixture, the total RNA was reversely transcribed. The mixture was kept in an incubator for 15 min at 37°C and then kept for 5 s at 85°C. The cDNA was kept at temperature of –20°C for future use.

Bmp38 and *BmS6K* Expression-Level Analysis Using Real-Time Quantitative Polymerase Chain Reaction

Real-time quantitative polymerase chain reaction (RT-qPCR) was performed for the examination of expression level of *Bmp38* and *BmS6K* in different tissues and under different post-treatments. The primers utilized in this study were designed by Primer Premier 5.0 (www.premierbiosoft.com; Table 1). According to the instructions of manufacturer, the real-time quantitative PCR were set with TB Green premix ex Taq (TaKaRa). Briefly, in a 25-µl reaction mixture, the RT-qPCR was performed containing 12.5-µl TB Green, 9.5-µl double-distilled water, 1-µl forward primer, 1-µl reverse primer, and 1-µl cDNA template. The thermal cycling program was set as follows: denaturation at temperature of 95°C for time period of 30 s, 40 cycles of temperature 95°C for 5 s, and 72°C for time of 20 s. Using the 96-well plates with multicolor RT–PCR detection system, the reactions were carried out (Bio-Rad). $2^{-\Delta\Delta Ct.}$ method was adopted according to the previously published protocol for the calculation of relative expression level (Yu et al. 2007). There were three biological sample replications. The *B. mori GAPDH* was used for normalization. ANOVA and LSD a posteriori tests were used for statistical analysis in SPSS software ($P < 0.05$).

Recombinant Protein Expression and Purification

Primers with restricted enzymes sites of EcoR I and Xho l were designed, the purpose of which was the amplification of Bmp38 and BmS6K domains for the recombinant protein expressions (Table 1). Using the pMD 19T vector, the PCR products (purified) were cloned as per previous protocol (Yu et al. 2017a). Positive colonies were randomly selected for sequencing DNA and for the confirmation of amplified sequence. Next, the plasmids were extracted, digested, purified, and ligated into the pET-28a vector (Novagen). The resulting recombinant plasmids pET-28a-*Bmp38* and *BmS6K* were confirmed by DNA sequencing and then transformed into *Escherichia coli* BL21 (DE3; Novagen) competent cells. After this activity, addition of isopropyl β-D-thiogalactoside was done and kept in an incubator for time period of 4 h at 37°C. The cells were harvested by centrifugation at 5,800 × *g* for 10 min. For cell pellets suspension, binding buffer (20 mM tris–HCl, 500 mM NaCl, 5 mM imidazole at pH 7.9) was used. This activity was then disrupted by sonication on ice. The procedure for recombinant proteins purification was used after centrifugation at 12,000 × *g* for time period of 20 min at temperature of 4°C by using a Ni-NTA Fast Start Kit (Qiagen, Inc., Valencia, CA) as per protocol of manufacturer. The quality and identity of purified proteins was evaluated. For this purpose, 12% sodium dodecyl sulfate–polyacrylamide gel electrophoresis (SDS–PAGE) and western blotting were performed by using anti-His primary antibody (Transgene Biotech, Beijing, China), and antigen–antibody complexes were detected with a horseradish peroxidase (HRP)-conjugated goat anti-mouse secondary antibody (Transgene Biotech; 1:5,000 dilution).

Preparation of Antibody and Western Blot

The recombinant Bmp38 and BmS6K proteins in purified form were submitted to HuaAn Biotechnology Ltd. (HUABIO, Hangzhou, China), to raise rabbit antibody as per protocol described by Yu et al. (2017a). Similarly, proteins for western blotting proteins were extracted from the various tissues of silkworms as per instructions of previous study (Yu et al. 2017a). Using a BCA protein assay kit (Bio-Rad) the purified proteins concentrations were quantified. In short, 12% SDS–PAGE gel was used for the separation of prepared protein samples (60 µg). It was then transferred into membranes of polyvinylidenedifluoride (PVDF). PVDF membrane was blocked overnight using 5% nonfat milk in PBST (137 mM NaCl, 2.7 mM KCl, 10 mM Na_2HPO_4, 2 mM K_2HPO_4, pH 7.5, 0.1% [v/v Tween-20]). It was washed three times with PBST, then used primary antibody (rabbit anti-Bmp38 and anti-BmS6K; diluted 1:5000), and incubated at room temperature for 2 h. Antigen–antibody complexes were detected after washing, with a horseradish peroxidase (HRP)-conjugated goat anti-rabbit secondary antibody (1:5,000 dilution; HUABIO, Hangzhou, China) in blocking buffer for time period of 1 h. Immobilized conjugates were visualized on membranes in HRP substrate solution (Tiangen, Beijing, China). GAPDH monoclonal antibody was used as control (Transgene Biotech).

Injection of Polyclonal Antibody Anti-Bmp38 and Anti-BmS6K

The purification of anti-Bmp38, anti-BmS6k serum, and preimmune serum was performed by the precipitation of ammonium sulfate according to previous method (Huang et al. 2015, Zhan et al. 2016). Protein concentrations were determined by Bradford reagent (Sangon Biotech, Shanghai, China). Western blotting showed that Bmp38 and BmS6K can be recognized by anti-Bmp38 and BmS6K serum. For further analysis, the efficacy of Bmp38 and BmS6K on BmNPV, anti-Bmp38/anti-BmS6K serum (0.5 mg/ml–5 µg/larvae), and preimmune serum (0.5 mg/ml–5 µg/larvae) was administered (injection) to abdomen of the first day of fifth instar of *B. mori* larvae. After 30 min, 10 microliters of BmNPV (BVs) suspended in water (1×10^5/ml) was administrated per os. All the experiments were performed in biological triplicates. Midgut tissues were obtained at 48 h postinfection

of BmNPV. Using genomic DNA extraction kit, the isolation of genomic DNA was performed (TaKaRa). Three BmNPV *GP41*, *IE-1*, and *GP64* genes were analyzed in *B. mori* midgut by RT-qPCR.

Results

BmNPV Proliferation Determination

To investigate the BmNPV infection characterization in silkworm, we monitored the dynamic proliferation of BmNPV in the midgut of the *B. mori*-resistant BC9 and -susceptible P50 strains by RT-qPCR. Melting curve analysis confirmed that specific amplification was achieved using a pair of primers against the BmNPV *GP41* gene. In the early stage after BmNPV infection (0–6 h), BmNPV proliferation was nearly undetected in the midgut-hypodermic injection and midgut-oral infection (Fig. 1). As the infection progressed, BmNPV copy numbers increased significantly from 13.9 to 1,746.7 within 6–48 h in the susceptible P50 midgut injected. In contrast, the BmNPV proliferation rate was low in the resistant BC9 midgut injected, which slowly increased to 683.2 at 48 hpi and 11,210.8 at 72 hpi. In the midgut oral, the relative copy numbers of *GP41* showed a similar pattern. The BmNPV copy numbers increased from 82.2 to 8,178.0 within 6–48 hpi in the susceptible P50. However, in resistant BC9, BmNPV proliferation was significantly slower with the relative copy number increasing from 6.5 to 2,216.2 within 6–48 hpi (Fig. 1). These results indicated that viral proliferation was faster in midgut oral than in midgut injected. In addition, we also found that 48 hpi was critical time point when BmNPV copy numbers showed a significant difference between resistant strain BC9 and susceptible stain P50.

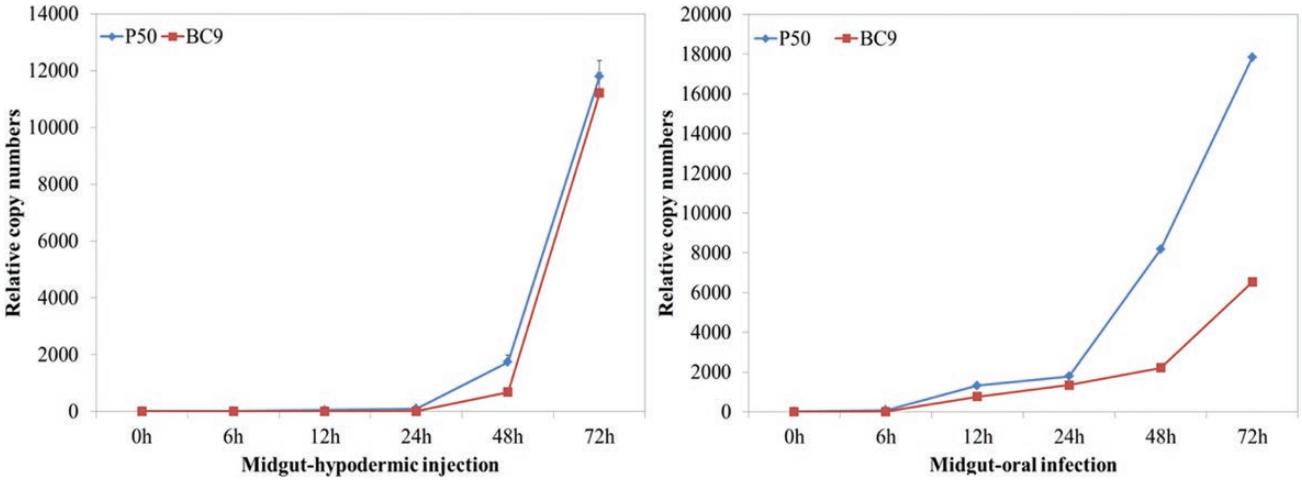

Fig. 1. The dynamic proliferation of BmNPV in the midgut of *Bombyx mori*-resistant BC9 and -susceptible P50 strains analyzed by RT-qPCR. A pair of primers against BmNPV *GP41* gene were used. Data were normalized using *BmGAPDH* and represented as mean ± SEM from three independent experiments. Relative expression levels were calculated using the $2^{-\Delta\Delta Ct}$ method.

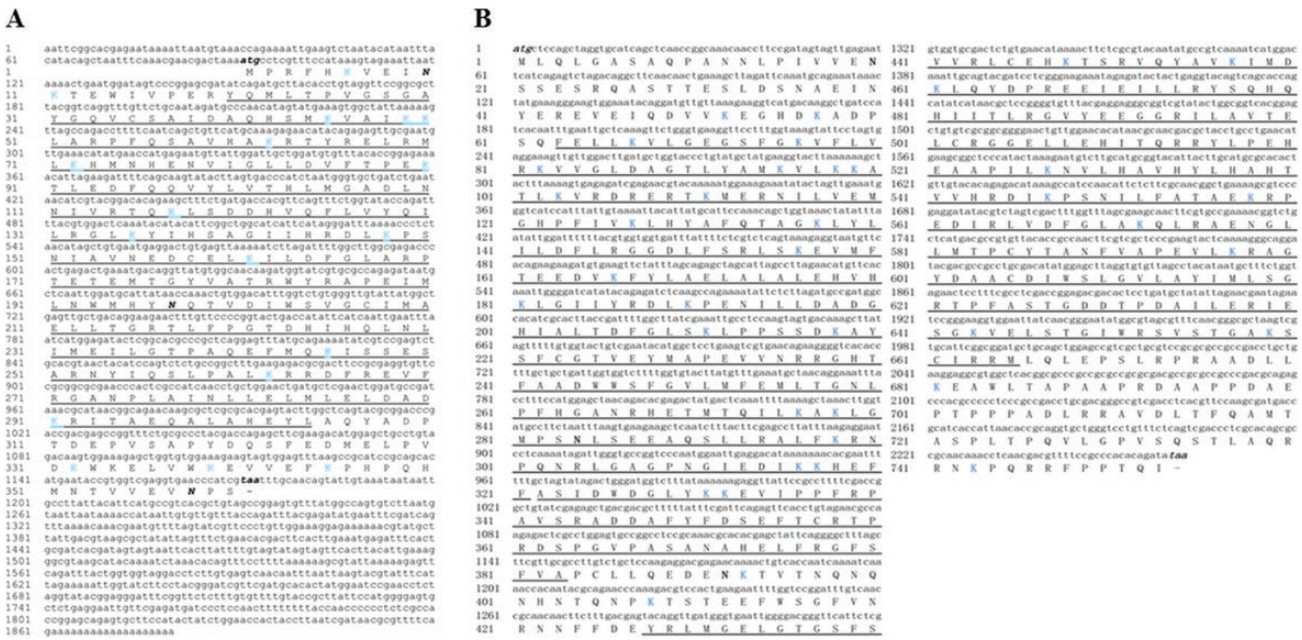

Fig. 2. The full-length cDNA sequence and its corresponding amino acid sequence of Bmp38 and BmS6K (A) and (B). The starts and stop codons are represented by bold italic letters. Numbers on the left side show position of nucleotides and amino acids. N-acetylation sites are represented by bold (N), whereas ubiquitination sites are shown by blue color (K). The domains are underlined.

Identification of Bmp38 and BmS6K, and Bioinformatics Analysis

The *Bmp38* (GenBank NM_001043531.1) and *BmS6K* (GenBank NM_001202528.1) were identified from transcriptome database of *B. mori* (Wang et al. 2016). The predicted full-length cDNA sequence of *Bmp38* consists of a 90 bp 5′ untranslated region (UTR), a 707 bp 3′ UTR, and 1,083 bp open reading frame (ORF) encoding 360 amino acids with theoretical MW of 41.55 kDa and IP of 5.93. The serine/threonine-protein kinases, catalytic domain (S_TKc) were identified at positions 20–304, with 3 N-glycosylation and 14 ubiquitination sites (Fig. 2A). The *BmS6K* cDNA contains 2,262 bp ORF encoding 753 amino acids with calculated MW of 84.5 kDa and IP of 6.45. No UTR was found in *BmS6K* cDNA sequence. Two S_TKc domains along with extension to Ser/Thr-type protein kinases domain (S_TK_x) were predicted in BmS6K amino acid sequence, with 3 N-glycosylation and 39 ubiquitination sites (Fig. 2B).

Multiple sequence alignment of Bmp38 and BmS6K with proteins of other organisms showed that Bmp38 and BmS6K include an activation loop, a conserved Thr-Glu-Tyr (TEY) and Thr-Leu-Tyr (TLY) phosphorylation motifs, respectively. Bmp38 has an ED site and a substrate-binding site. Pairwise sequence analysis of Bmp38 protein sequence shows 84.8, 91.2, 98.3, and 70.3% similarity with

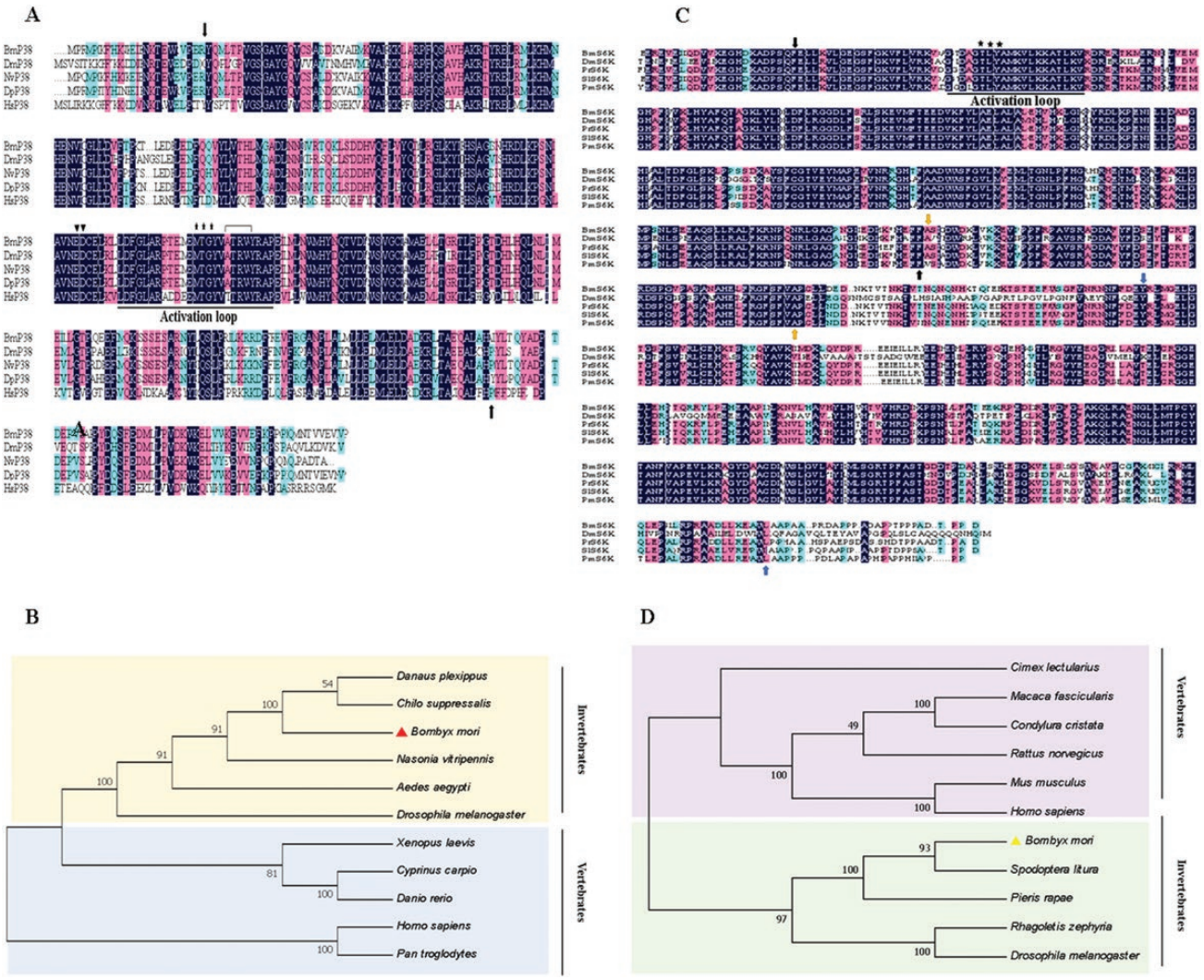

Fig. 3. (A) Multiple sequences alignment of Bmp38 with other known organisms p38 homolog. A hundred percent conserved amino acids are shaded in black. The domain is represented by black arrows. The activation loop is underlined, ED site is shown by inverted triangles, TGY motif is shown by stars, and substrate site is represented by inverted bracket. Organisms used for multiple sequence alignment are *Bombyx mori* (NP_001036996.1), *Drosophila melanogaster* (AAB97138.1), *Nasonia vitripennis* (XP_001136337.1), *Danaus plexippus plexippus* (OWR52323.1), and *Homo sapiens* (AAC51758.1). (B) Multiple sequences alignment of BmS6K with other known organisms S6K homolog. The positions of three different domains are shown by different colors arrows (black, yellow, and blue). The activation loop is underlined, TYL motif is shown by stars. *Bombyx mori* (NP_001189457.1), *D. melanogaster* (AAA50509.1), *Pieris rapae* (XP_022122087), *Spodoptera litura* (XP_022827882.1), and *Papilio machaon* (KPJ06800.1) were used for alignment. (C) Phylogenetic tree of Bmp38 with other organisms. *Bombyx mori* p38 is shown with red color triangle. Organisms used to construct p38 phylogenetic tree are *B. mori* (NP_001036996.1), *D. melanogaster* (AAB97138.1), *Aedes aegypti* (XP_001653239.1), *N. vitripennis* (XP_001136337.1), *D. p. plexipus* (OWR52323.1), *Rattus norvegicus* (AAB51285.1), *H. sapiens* (AAC51758.1), *Pan troglodytes* (NP_00102926.1), *Chilo suppressalis* (AN046359.1), *Xenopus laevis* (NP_001165343.1), *Cyprinus carpio* (BAA96415.1), and *Danio rerio* (NP_571797.1). (D) Phylogenetic tree of BmS6K with other organisms. *Bombyx mori* S6K is shown with yellow color triangle. Organisms used to construct phylogenetic trees are *B. mori* (NP_001189457.1), *D. melanogaster* (AAA50509.1), *R. norvegicus* (NP_112369.1), *Cimex lectularis* (XP_024085928.1), *Macaca fascicularis* (XP_005593208.1), *Condylura cristata* (XP_004689960.1), *Mus musculus* (NP_035429.1), *H. sapiens* (BAD92353.1), *S. litura* (XP_022827882.1), *Pieris rapae* (XP_022122087), and *Rhagoletis zephyria* (XP_ 017483318.1).

Drosophila melanogaster, *Nasonia vitripennis*, *Danaus plexippus plexippus*, and *Homo sapiens*, respectively. Similarly, the BS6K protein sequence shows 58.9, 91.5, 94.5, and 85.9% similarity with *D. melanogaster*, *Pieris rapae*, *Spodoptera litura*, and *Papilio machaon* (Fig. 3A–C).

To explore the evolutionary relationship of Bmp38 and BmS6K, a phylogenic tree was constructed by the neighbor-joining method from p38 and S6K proteins of different species. The phylogenetic tree can be classified into vertebrates and invertebrates. Bmp38 was closely related to *Chilo suppressalis* and *D. plexippus*, and BmS6K protein showed close relationship with *S. litura* and *P. rapae* (Fig. 3B and C). Based on iTRAQ database, Bmp38 and BmS6K were identified as differentially expressed proteins in different silkworm strains P50 (susceptible strain) and BC9 (resistant strain) according to iTRAQ database (Yu et al. 2017b). Based on iTRAQ database, Bmp38 and BmS6K expressions were upregulated in P50+ and BC9+ infected with BmNPV than P50– and BC9– noninfected. The expression of both proteins was upregulated in resistant strain of silkworm BC9 after BmNPV infection data obtained from iTRAQ database (Table 2).

Recombinant Protein Expression, Purification, and Antibody Preparation

To analyze the physiological function of Bmp38 and BmS6K proteins, recombinant His-tagged Bmp38 and BmS6K were expressed using prokaryotic expression system. The recombinant proteins (Bmp38 and BmS6K) were successfully expressed and detected by SDS–PAGE with molecular mass of approximately 35kDa and 30kDa, respectively (Fig. 4A–C). The recombinant proteins were purified under denaturing conditions by affinity chromatography using Ni-NTA column (Fig. 4B–D), and recombinant proteins were confirmed through western blotting (Fig. 5). For preparation of antibody, purified proteins were utilized. The titer of antibody was 1:60,000 approximately as per ELISA determination.

Table 2. Differentially expressed proteins Bmp38 and BmS6K identified by iTRAQ in silkworm different strains P50 (susceptible strain) and BC9 (resistant strain) following BmNPV infection

Protein name	P50–	P50+	BC9–	BC9+	P50+ vs. P50–	BC9+ vs. BC9–
Bmp38	0.98978103	1.042841056	0.842422284	1.090504407	1.053608	1.294487
BmS6K	1.071713236	1.007657633	0.866446491	1.076495041	0.940231	1.242425

BmNPV (*Bombyx mori* nucleopolyhedrovirus).

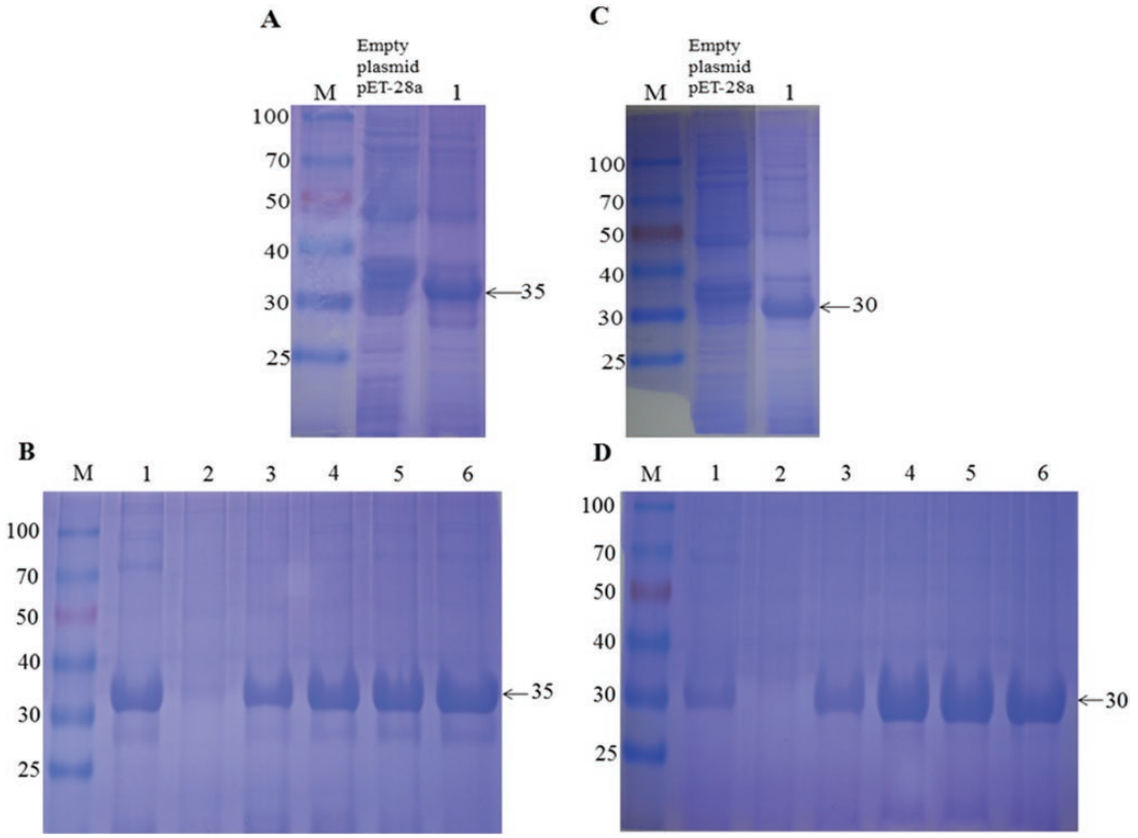

Fig. 4. Prokaryotic expression of recombinant proteins Bmp38 (A) and BmS6K (C) on sodium dodecyl sulfate–polyacrylamide gel electrophoresis (SDS–PAGE) with isopropyl β-D-thiogalactoside. M: protein marker, empty plasmid pET-28a, was used as negative control. Lane 1, target recombinant protein. Recombinant protein purification of Bmp38 (B) and BmS6K (D) on SDS–PAGE. M: protein maker, Lane 1: effluent liquid, Lane 2: washing liquid, and Lane 3–6: elution liquid (contain 250 mM imidazole).

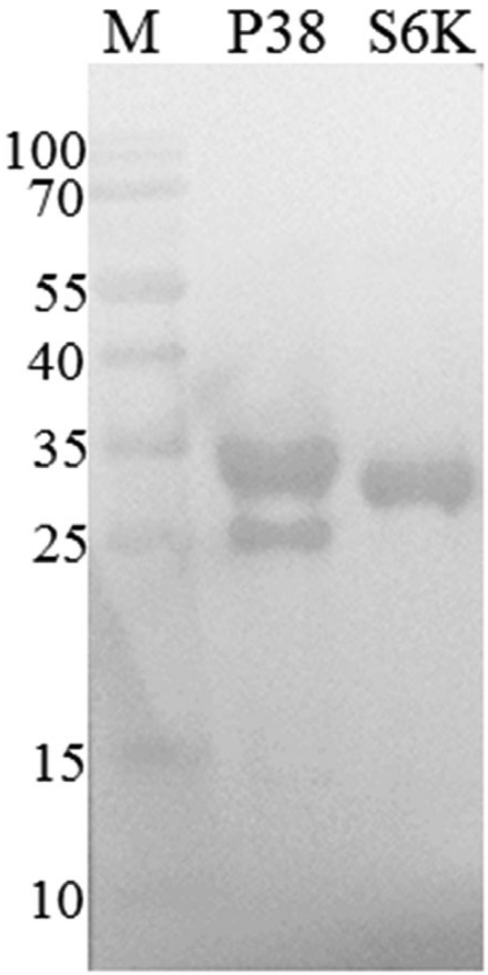

Fig. 5. Western blot analysis of recombinant His-tagged Bmp38 and BmS6K proteins identified by anti-His antibodies. M: protein marker. P38: Bmp38 and S6K: BmS6K.

Tissue Distribution of Bmp38 and BmS6K in Different Silkworm Strains After BmNPV Infection

To analysis tissue distribution of Bmp38 and BmS6K, different tissues including hemolymph, fat body, integument, head, midgut, and silk gland were collected for P50 and BC9 at 72 h after BmNPV challenge. After this, the RT-qPCR and western blot were performed. The *Bmp38* was consecutively expressed in every tissue examined, with higher expression in the midgut, followed by the hemolymph. Furthermore, the *Bmp38* expression levels in P50 (susceptible strain) and BC9 (resistant strain) were upregulated in the midgut, silk gland, integument, and hemolymph after BmNPV infection, whereas its expression level was downregulated in the fat body and head for P50 and was upregulated for BC9 after BmNPV infection (Fig. 6A). Western blot results also showed that Bmp38 expression was relatively higher in the midgut, hemolymph, and fat body, which also validated our RT-qPCR results. However, no obvious hybrid band for Bmp38 was detected in the integument according to western blotting (Fig. 6B).

The RT-qPCR results indicated that *BmS6K* showed a different expression pattern with *Bmp38*. The *BmS6K* expression was also observed in every tissue examined, with the highest expression level in the hemolymph and midgut. The lowest expression was observed in the silk gland. Interestingly, unlike *Bmp38*, the expression between P50 (susceptible strain) and BC9 (resistant strain) of *BmS6K* was similar in the hemolymph and midgut, which was upregulated in P50 and BC9 after BmNPV infection. *BmS6K* expression level was downregulated in the head after BmNPV infection (Fig. 6C). The translation level of BmS6K exposed that BmS6K had comparatively higher expression levels in the head, followed by the fat body. The translation data confirmed that BC9 had higher expression than P50 in the fat body after BmNPV infection (Fig. 6D).

Expression Profile of Bmp38 and BmS6K at Different Time Points After Challenging With BmNPV

To evaluate iTRAQ database, we obtained the expression profile of Bmp38 and BmS6K in the midgut infected with BmNPV, and results were evaluated by RT-qPCR and western blotting. The RT-qPCR results of Bmp38 indicated that its expression was upregulated in infected group (P50+ and BC9+) than control group (P50– and BC9–). When compared between P50 (susceptible strain) and BC9 (resistant strain), we observed that Bmp38 expression was higher in BC9 more than P50 at 12, 24, 48, and 72 h (Fig. 7A). In addition, western blot results showed that Bmp38 translation profile is correlated with Bmp38 transcription profile (Fig. 7B).

In case of *BmS6K*, the expression was upregulated in infected group (P50+ and BC9+) than control group (P50– and BC9–). However, BC9 expression was slightly increased at 6 h, then dramatically increased at 12, 24, 48, and 72 h than P50 after BmNPV infection (Fig. 7C). The western blot analysis also confirmed that the expression of BmS6K was upregulated after BmNPV infection (Fig. 7D).

Effects on Viral Proliferation of Antibody Blocking of Bmp38 and BmS6K

The translation and transcription profiles of Bmp38 and BmS6K exposed that their expression was higher in BC9 (resistant strain). Next, we analyzed the effect of Bmp38 and BmS6K in BC9 through blocking with antibody on virus proliferation. We injected anti-Bmp38/anti-BmS6K serum, preimmune serum, and CK to silkworm (*B. mori*). After 30 min, BmNPV (1×10^5/ml) suspension per os was orally administered. RT-qPCR was performed to analysis the relative copy number of viral genes *GP41*, *IE-1*, and *GP64*. The results indicated that after blocking of Bmp38 with anti-Bmp38, relative copy number of viral genes were upregulated than preimmune serum and CK (Fig. 8A). However, blocking of BmS6K with anti-BmS6K showed that relative copy number of viral genes was significantly upregulated than CK, but significantly downregulated than preimmune serum (Fig. 8B).

Discussion

MAPK signaling pathways are evolutionarily conserved Ser–Thr kinases with a wide range of biological functions. MAPKs consist of three subfamilies including ERK, JNK, and p38 MAPK (Johnson and Lapadat 2002, Roux and Blenis 2004, Huang et al. 2009). The activation of MAPKs depends on phosphorylation of certain motifs found in activation loop. The p38 MAPK and S6K are important proteins of MAPK family. Evidence showed that p38 MAPK and S6K play vital role in both vertebrates and invertebrates (Roux and Blenis 2004, Fenton and Gout 2011). However, studies on p38 and S6K MAPK proteins in silkworm had not been reported previously. Therefore, in the present study, we identified *B. mori* p38 and S6K proteins from iTRAQ database. The sequence analysis showed that Bmp38 and BmS6K contain S_TKc domain with 360 aa and 753 aa, respectively. Multiple sequence alignment of Bmp38 and BmS6k

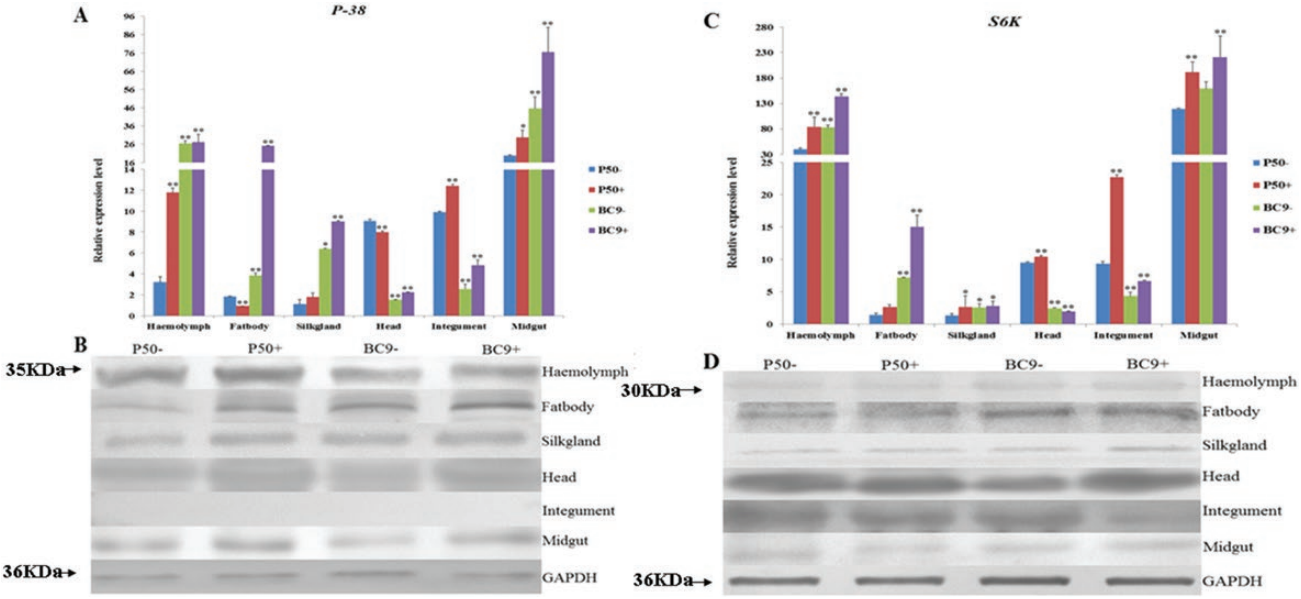

Fig. 6. Relative expression pattern of *Bmp38* (A) and *BmS6K* (C) in different tissues of different resistant silkworm strains following BmNPV infection for 72 h. Data were normalized using *BmGAPDH* and represented as mean ± SEM from three independent experiments. Relative expression levels were calculated using the $2^{-\Delta\Delta Ct}$ method. Statistical analysis was performed using SPSS software. The significant difference was indicated by $^{*}P < 0.05$ or $^{**}P < 0.01$. Immunoblotting results of Bmp38 (B) and BmS6K (D) in the different tissues of different resistant silkworm strains following BmNPV infection for 72 h. GAPDH antibody was used as control.

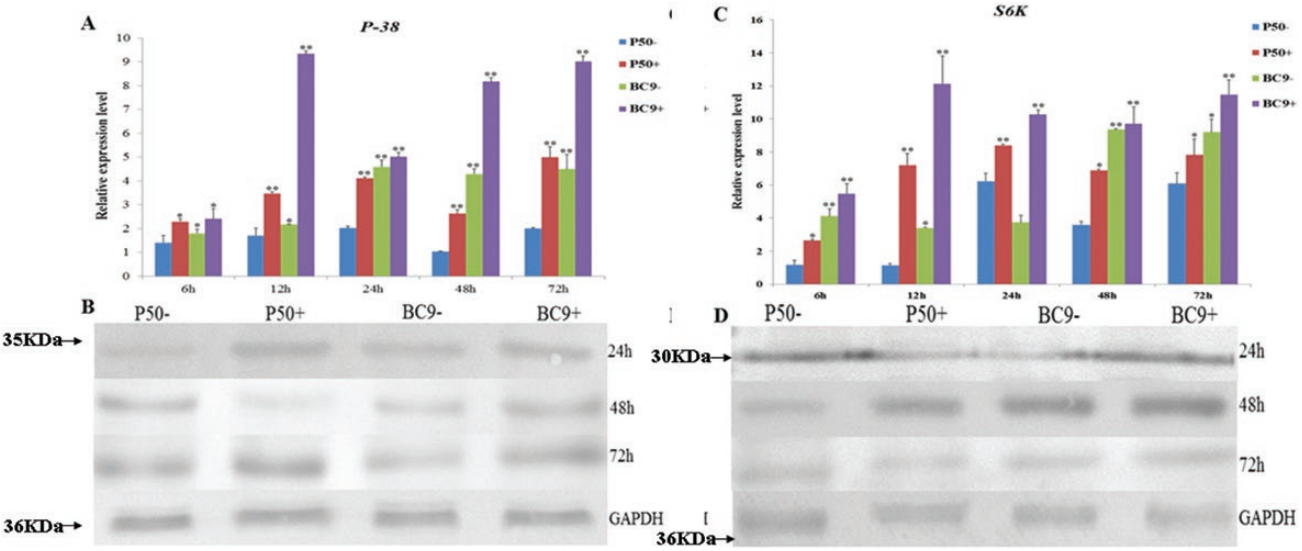

Fig. 7. Relative expression level of *Bmp38* (A) and *BmS6K* (C) in the midgut of different resistant silkworm strains following BmNPV infection for 6, 12, 24, 48, and 72 h. Data were normalized using *BmGAPDH* and represented as mean ± SEM from three independent experiments. Relative expression levels were calculated using the $2^{-\Delta\Delta Ct}$ method. Statistical analysis was performed using SPSS software. The significant difference was indicated by $^{*}P < 0.05$ or $^{**}P < 0.01$. Immunoblotting results of Bmp38 (B) and BmS6K (D) in the midgut of different resistant silkworm strains following BmNPV infection for 24, 48, and 72 h. GAPDH antibody was used as control.

with other organisms (having known functions) revealed common features in all of them, e.g., activation loop and motifs. The phylogenetic analysis provided evidences that Bmp38 and BmS6K homologous are highly conserved in vertebrates and invertebrates. This phylogenetic analysis is consistent with the previous studies (Lin et al. 2017, Yu et al. 2017c).

Previous reports indicate that p38 MAPK signaling involved in the cellular immune responses in mammals (Hoefen and Berk 2002). In *Drosophila*, the p38 MAPK participate in host defense and protect *Drosophila* form injury caused by pathogens (Chen et al. 2010). A p38 MAPK from *Litopenaeus vannamei* gene expression showed upregulation when challenged with pathogens (Yan et al. 2013). Studies have shown that p38 MAPK participates in viral replication in in vito (Johnson et al. 2000, Khatri and Sharma 2006). In this study, to determine Bmp38 can participate in immune response of *B. mori*, we analyzed Bmp38 expression after BmNPV infection. Our study results showed that *Bmp38* expression was higher in the midgut, followed by the hemolymph after BmNPV infection. The

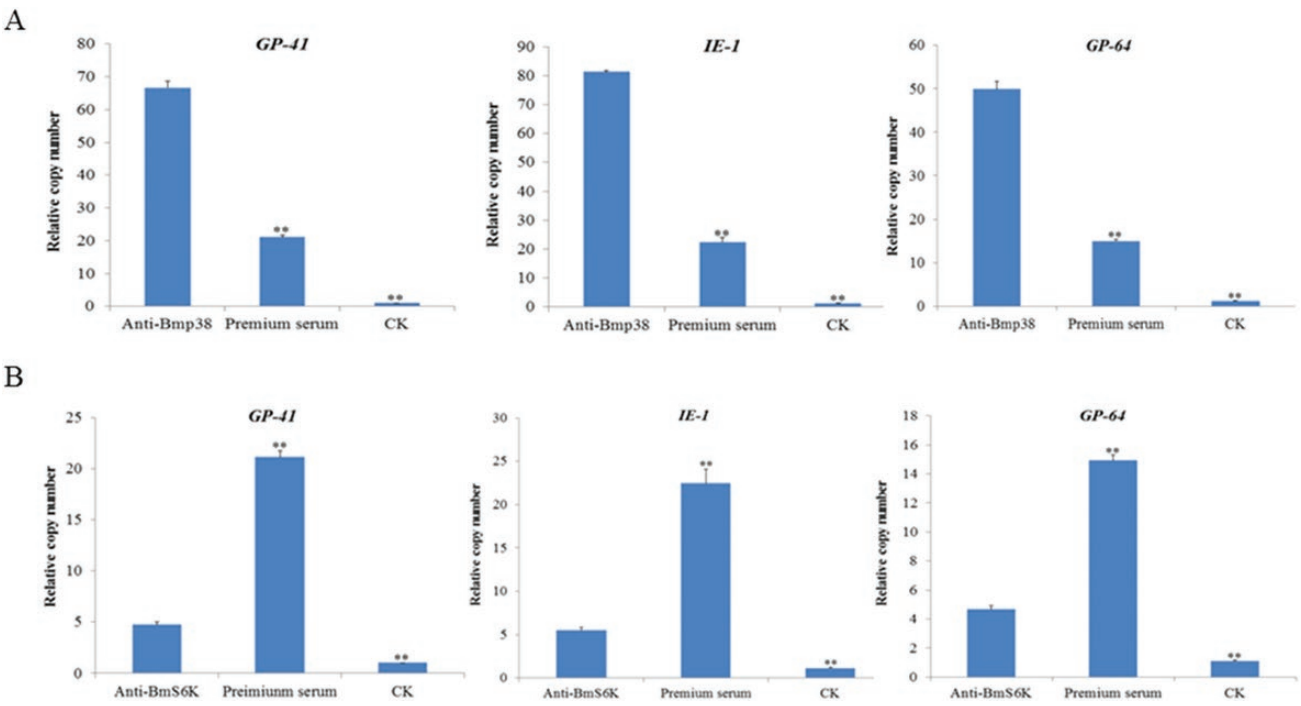

Fig. 8. Relative expression level of viral genes copy number *GP41*, *IE-1*, and *GP64* after antibody blocking of Bmp38 (A) and BmS6K (B). Preimmune serum and CK were used as control. Data were normalized using *BmGAPDH* and represented as mean ± SEM from three independent experiments. Relative expression levels were calculated using the $2^{-\Delta\Delta Ct}$ method. Statistical analysis was performed using SPSS software. The significant difference was indicated by $*P < 0.05$ or $**P < 0.01$.

expression in different silkworm strains showed that *Bmp38* expression was upregulated in BC9 (resistant strain) than P50 (susceptible strain). The translation data confirmed that Bmp38 expression was higher in the BC9 than in the P50. We also observed the expression of Bmp38 in the midgut post-BmNPV infection. The results showed that *Bmp38* expression was upregulated in P50+ and BC9+ than control. Moreover, expression in the BC9 was higher than P50 after BmNPV infection. Immunoblot results confirmed that Bmp38 expression was higher in the BC9 than in the P50. These findings are in accordance with our previous iTRAQ database (Yu et al. 2017b). Similar evidence from different organisms showed *p38* MAPK signaling pathway mRNA expression was increased after pathogen infection (He et al. 2013, 2018; Yan et al. 2013; Zhu et al. 2014). A p38 protein from *Scylla paramamosain* showed that it is involved in immune response against bacteria and virus (Yu et al. 2017c). These findings suggest that Bmp38 may be involved in immune response against BmNPV.

Ribosomal S6 kinase is a central component in the TOR pathway to regulate cell growth and energy metabolism in animals (Fenton and Gout 2011). The study on S6K in *Drosophila* suggests that disruption of S6K cause the death of flies at the larvae and pupa stage (Montagne et al. 1999). To date, there are no reports on S6K functions against pathogens. We observed the transcription and translation level of *B. mori* S6K. Our results showed that *BmS6K* expression was higher in the hemolymph and midgut after BmNPV infection. The translation results showed that BmS6K expression was higher in the head, followed by the fat body. The transcription results of *BmS6K* in the midgut after BmNPV infection revealed that *BmS6K* expression was at peak at 12 h postinfection, then its expression decreased slightly at 24, 48, and 72 h, but it was still significantly upregulated. The translation data also correlate with the transcription data. Moreover, we found that BmS6K translation data are somewhat consistent with the iTRAQ and need further attention.

For further confirmation of Bmp38 and BmS6K role in silkworm against BmNPV infection, we used BC9 (resistant strain) and blocked the proteins with corresponding antibodies. The results indicated that Bmp38 blocking increased the relative copy numbers of viral genes when compared with control. It has been reported that silence of p38 from Chinese shrimp (*Fenneropenaeus chinensis*) revealed its role against white spot syndrome virus (He et al. 2018). Pharmacological inhibition of p38 MAPK by SB203580 affected the replication of influenza virus and respiratory syncytial virus (Marchant et al. 2010). Therefore, we speculated that Bmp38 might be involved in BmNPV resistance. The RSK family comprised a group of highly related serine/threonine kinases that regulated diverse cellular processes, including proliferation, cell growth, and motility. Members of RSK family contained RSK1, RSK2, RSK3, and RSK4. Among them, activated RSK2 was shown to phosphorylate several transcription factors response to viral infection (Yan et al. 2018). Surviladze et al. (2013) revealed that activation of PI3K/Akt/mTOR could phosphorylate S6K to further activate the downstream signal pathways in response to human papillomavirus type 16 infection. In case of BmS6K, the relative copy numbers of viral genes were significantly upregulated than CK. We considered that BmNPV resistance of BmS6K required phosphorylation modification. Therefore, the specific reasons need to be conducted. The abovementioned results suggested that blocking of Bmp38 and BmS6K in BC9 (resistant strain) might participate in BmNPV proliferation.

In summary, the p38 and S6K proteins from *B. mori* were characterized for the first time. The expression profiles of Bmp38 and BmS6K showed that they might play vital role in silkworm against BmNPV infection. The study presented here would enhance further investigation of silkworm immune defense against BmNPV infection.

Acknowledgments

This work was supported by National Natural Science Foundation of China (31472148) and Anhui International Joint Research and Developmental Center of Sericulture Resources Utilization (2017R0101).

References Cited

Banerjee, S., K. Narayanan, T. Mizutani, and S. Makino. 2002. Murine of stress-responsive genes after challenge with viruses and temperature coronavirus replication-induced p38 mitogen-activated protein kinase activation promotes interleukin-6 production and virus replication in cultured cells. J. Virol. 76: 5937–5948.

Chen, J., C. Xie, L. Tian, L. Hong, X. Wu, and J. Han. 2010. Participation of the p38 pathway in *Drosophila* host defense against pathogenic bacteria and fungi. Proc. Natl. Acad. Sci. USA 107: 20774–20779.

Fenton, T. R., and I. T. Gout. 2011. Functions and regulation of the 70 kDa ribosomal S6 kinases. Int. J. Biochem. Cell Biol. 43: 47–59.

Guo, H., L. Jiang, and Q. Xia. 2016. Selection of reference genes for analysis changes in the silkworm *Bombyx mori*. Mol. Genet. Genomics 291: 999–1004.

Gwalter, J., M. L. Wang, and I. Gout. 2009. The ubiquitination of ribosomal S6 kinases is independent from the mitogen-induced phosphorylation/activation of the kinase. Int. J. Biochem. Cell Biol. 41: 828–833.

Han, Z. S., H. Enslen, X. Hu, X. Meng, I. H. Wu, T. Barrett, R. J. Davis, and Y. T. Ip. 1998. A conserved p38 mitogen-activated protein kinase pathway regulates *Drosophila* immunity gene expression. Mol. Cell. Biol. 18: 3527–3539.

He, S., Z. Qian, J. Yang, X. Wang, X. Mi, Y. Liu, F. Hou, Q. Liu, and X. Liu. 2013. Molecular characterization of a p38 MAPK from *Litopenaeus vannamei* and its expression during the molt cycle and following pathogen infection. Dev. Comp. Immunol. 41: 217–221.

He, Y., W. Yao, P. Liu, J. Li, and Q. Wang. 2018. Expression profiles of the p38 MAPK signaling pathway from Chinese shrimp *Fenneropenaeus chinensis* in response to viral and bacterial infections. Gene 642: 381–388.

Hirasawa, K., A. Kim, H. S. Han, J. Han, H. S. Jun, and J. W. Yoon. 2003. Effect of p38 mitogen-activated protein kinase on the replication of encephalomyocarditis virus. J. Virol. 77: 5649–5656.

Hoefen, R. J., and B. C. Berk. 2002. The role of MAP kinases in endothelial activation. Vascul. Pharmacol. 38: 271–273.

Huang, G., L. Z. Shi, and H. Chi. 2009. Regulation of JNK and p38 MAPK in the immune system: signal integration, propagation and termination. Cytokine 48: 161–169.

Huang, W., X. Xu, S. Freed, Z. Zheng, S. Wang, S. Ren, and F. Jin. 2015. Molecular cloning and characterization of a beta-1,3-glucan recognition protein from *Plutella xylostella* (L.). New Biotechnol. 32: 290–299.

Johnson, G. L., and R. Lapadat. 2002. Mitogen-activated protein kinase pathways mediated by ERK, JNK, and p38 protein kinases. Science 298: 1911–1912.

Johnson, R. A., S. M. Huong, and E. S. Huang. 2000. Activation of the mitogen-activated protein kinase p38 by human cytomegalovirus infection through two distinct pathways: a novel mechanism for activation of p38. J. Virol. 74: 1158–1167.

Kakugawa, S., M. Shimojima, H. Goto, T. Horimoto, N. Oshimori, G. Neumann, T. Yamamoto, and Y. Kawaoka. 2009. Mitogen-activated protein kinase-activated kinase RSK2 plays a role in innate immune responses to influenza virus infection. J. Virol. 83: 2510–2517.

Khatri, M., and J. M. Sharma. 2006. Infectious bursal disease virus infection induces macrophage activation via p38 MAPK and NF-kappaB pathways. Virus Res. 118: 70–77.

Kuang, E., Q. Tang, G. G. Maul, and F. Zhu. 2008. Activation of p90 ribosomal S6 kinase by ORF45 of Kaposi's sarcoma-associated herpesvirus and its role in viral lytic replication. J. Virol. 82: 1838–1850.

Lin, Q., J. Fan, L. Liu, B. Zhang, X. Wang, C. Lei, Y. Lin, and W. Ma. 2017. Knockdown of the MAPK p38 pathway increases the susceptibility of *Chilo suppressalis* larvae to *Bacillus thuringiensis* Cry1Ca toxin. Sci. Rep. 7: 43964.

Marchant, D., G. K. Singhera, S. Utokaparch, T. L. Hackett, J. H. Boyd, Z. Luo, X. Si, D. R. Dorscheid, B. M. McManus, and R. G. Hegele. 2010. Toll-like receptor 4-mediated activation of p38 mitogen-activated protein kinase is a determinant of respiratory virus entry and tropism. J. Virol. 84: 11359–11373.

Marie Cargnello, P. P. R. 2011. Activation and Function of the MAPKs and Their Substrates, the MAPK-activated protein kinases. Microbio. Mol. Biol. Rev. 75: 50–83.

Montagne, J., M. J. Stewart, H. Stocker, E. Hafen, S. C. Kozma, and G. Thomas. 1999. *Drosophila S6 kinase*: a regulator of cell size. Science 285: 2126–2129.

Regan, A. D., R. D. Cohen, and G. R. Whittaker. 2009. Activation of p38 MAPK by feline infectious peritonitis virus regulates pro-inflammatory cytokine production in primary blood-derived feline mononuclear cells. Virology 384: 135–143.

Roux, P. P., and J. Blenis. 2004. ERK and p38 MAPK-activated protein kinases: a family of protein kinases with diverse biological functions. Microbiol. Mol. Biol. Rev. 68: 320–344.

Shahzad, T., M. Y. Zhan, P. J. Yang, X. Q. Yu, and X. J. Rao. 2017. Molecular cloning and analysis of a C-type lectin from silkworm *Bombyx mori*. Arch. Insect Biochem. Physiol. 95: e21391.

Surviladze, Z., R. T. Sterk, S. A. DeHaro, and M. A. Ozbun. 2013. Cellular entry of human papillomavirus type 16 involves activation of the phosphatidylinositol 3-kinase/Akt/mTOR pathway and inhibition of autophagy. J. Virol. 87: 2508–2517.

Tamura, K., G. Stecher, D. Peterson, A. Filipski, and S. Kumar. 2013. MEGA6: Molecular Evolutionary Genetics Analysis, version 6.0. Mol. Biol. Evol. 30: 2725–2729.

Tavares, M. R., I. C. Pavan, C. L. Amaral, L. Meneguello, A. D. Luchessi, and F. M. Simabuco. 2015. The S6K protein family in health and disease. Life Sci. 131: 1–10.

Wang, X. Y., H. Z. Yu, L. Geng, J. P. Xu, D. Yu, S. Z. Zhang, Y. Ma, and D. Q. Fei. 2016. Comparative transcriptome analysis of *Bombyx mori* (Lepidoptera) larval midgut response to BmNPV in susceptible and near-isogenic resistant strains. PLoS One 11: e0155341.

Wang, X. Y., H. Z. Yu, J. P. Xu, S. Z. Zhang, D. Yu, M. H. Liu, and L. L. Wang. 2017. Comparative subcellular proteomics analysis of susceptible and near-isogenic resistant *Bombyx mori* (Lepidoptera) larval midgut response to BmNPV infection. Sci. Rep. 7: 45690.

Wei, S., Y. Huang, X. Huang, and Q. Qin. 2015. Characterization of c-Jun from orange-spotted grouper, *Epinephelus coioides* involved in SGIV infection. Fish Shellfish Immunol. 43: 230–240.

Xia, Q., Z. Zhou, C. Lu, D. Cheng, F. Dai, B. Li, P. Zhao, X. Zha, T. Cheng, C. Chai, et al.; Biology Analysis Group. **2004**. A draft sequence for the genome of the domesticated silkworm (*Bombyx mori*). Science 306: 1937–1940.

Yan, H., S. Zhang, C. Z. Li, Y. H. Chen, Y. G. Chen, S. P. Weng, and J. G. He. 2013. Molecular characterization and function of a p38 MAPK gene from *Litopenaeus vannamei*. Fish Shellfish Immunol. 34: 1421–1431.

Yan, L. B., Y. J. Yu, Q. B. Zhang, X. Q. Tang, L. Bai, F. Huang, and H. Tang. 2018. Identification of p90 ribosomal S6 Kinase 2 as a novel host protein in HBx augmenting HBV replication by iTRAQ-based quantitative comparative proteomics. Proteomics Clin. Appl. 12: e1700090.

Yee, A. S., E. K. Paulson, M. A. McDevitt, K. Rieger-Christ, I. Summerhayes, S. P. Berasi, J. Kim, C. Y. Huang, and X. Zhang. 2004. The HBP1 transcriptional repressor and the p38 MAP kinase: unlikely partners in G1 regulation and tumor suppression. Gene 336: 1–13.

Yu, S., H. Liu, and L. Luo. 2007. Analysis of relative gene expression using different real-time quantitative PCR. Acta Agrono. Sini. 7: 1214–1218.

Yu, H.-Z., S.-Z. Zhang, Y. Ma, D.-Q. Fei, B. Li, L.-A. Yang, J. Wang, Z. Li, A. Muhammad, and J.-P. Xu. 2017a. Molecular characterization and functional analysis of a ferritin heavy chain subunit from the Eri-silkworm, *Samia cynthia ricini*. Int. J. Mol. Sci. 18: 2126.

Yu, H., X. Wang, J. Xu, Y. Ma, S. Zhang, D. Yu, D. Fei, and A. Muhammad. 2017b. iTRAQ-based quantitative proteomics analysis of molecular

mechanisms associated with *Bombyx mori* (Lepidoptera) larval midgut response to BmNPV in susceptible and near-isogenic strains. J. Proteomics 165: 35–50.

Yu, Z., Y. Geng, A. Huang, K. Wang, X. Huang, D. Chen, Y. Ou, and J. Wang. 2017c. Molecular characterization of a p38 mitogen-activated protein kinase gene from *Scylla paramamosain* and its expression profiles during pathogenic challenge. J. Invertebr. Pathol. 144: 32–36.

Yu, H. Z., J. Wang, S. Z. Zhang, S. Toufeeq, B. Li, Z. Li, L. A. Yang, P. Hu, and J. P. Xu. 2018. Molecular characterisation of *Apolipophorin-III* gene in *Samia cynthia ricini* and its roles in response to bacterial infection. J. Invertebr. Pathol. 159: 61–70.

Zhan, M. Y., T. Shahzad, P. J. Yang, S. Liu, X. Q. Yu, and X. J. Rao. 2016. A single-CRD C-type lectin is important for bacterial clearance in the silkworm. Dev. Comp. Immunol. 65: 330–339.

Zhu, J., L. Cai, T. Zhang, L. Chen, P. Jin, and F. Ma. 2014. Identification and characterization of a p38-like gene from amphioxus (*Branchiostoma belcheri*): an insight into amphioxus innate immunity and evolution. Fish Shellfish Immunol. 41: 421–427.